

## **Influence of pressure on the mechanical properties and grain refinement of die cast aluminum A1350 alloy**

**Obiekea K., Aku S.Y and Yawas D.S**

*Department of Mechanical Engineering, Ahmadu bello University, Zaria, Kaduna State, Nigeria*

---

### **ABSTRACT**

*An experimental study on the “the influence of pressure on the mechanical properties and grain refinement of die cast aluminum A1350 alloy” was carried out and subsequent analysis made. The results obtained from the microstructure analyses carried out on the A1350 alloy cast samples show that structural changes occurred as different morphologies of grains size and numbers were observed under the different applied pressures in the castings as some appeared granular, lamella, coarse e.tc. also the mechanical properties like the tensile, impact strength and hardness all showed variations under different pressures in the castings as the hardness increased with applied pressure from 77 to 86 HRN and tensile, yield strengths and elongation of the cast samples varied as maximum values were observed with applied pressures of 1400kg/cm<sup>2</sup> and the impact strength increased with applied pressures from 3.98 to 4.44 joules. Microstructure refining caused by more number of grains and finer grain sizes was observed in the micrograph in the sample at applied pressure of 1400kg/cm<sup>2</sup> and porosity was not found due to microstructure refining as compared with those obtained at 0 kg/cm<sup>2</sup> and 700kg/cm<sup>2</sup> These results illustrate how the influence of pressure on the grain refinement and mechanical properties can be used to improve the qualities of die cast products.*

---

### **INTRODUCTION**

Most recently, pressure die cast (PDC) aluminum alloys have played a significant role in the renovation of historic buildings [1]. The characteristics and properties of PDC aluminum as a material have led to revolutionary and innovative changes in building techniques, architectural and engineering projects.

Re-melting used aluminum requires only 5 per cent of the energy needed to produce the primary metal. Thus, rather than contributing to society’s growing waste problem, aluminum can be re-melted and reformed to produce a new generation of parts. Aluminum in general has always been recycled at a higher rate than most other raw materials. Given the necessary infrastructure, it is possible to recycle all aluminum in construction industry applications, for several reasons. First, there is a relatively high level of scrap aluminum available. Second, aluminum has a high scrap value, which can contribute significantly towards covering demolition costs. Finally, the infrastructure required for the collection of scrap metals is already well established and will continue to grow on its own economic merit as it has done in the past to provide an increasingly efficient recycling system.

Nearly 40 per cent of all aluminum used today is re-melted metal [1]. In addition, all the standards that have been set for using of metal components, die cast aluminum alloys satisfy these standards to the utmost. Hence, they are certified safe for use (ISO 9001).

Cost savings in castings are achieved by producing the lightest parts possible to perform the job to be done. Today there is an increasing trend in the industry towards alloys that provide increased strength over traditional alloys. In order to determine whether the casting process produces a part with proper as-cast mechanical properties, microstructure prediction is required. Microstructure of metals is a useful tool in the sense that it indicates casting defects .

Researchers like Ming et al [2] conducted experiments on the effect of pressure on the mechanical properties and microstructure of Al-Cu-based alloy prepared by squeeze casting and concluded that hardness, tensile strength and ductility of ZA27 squeezed casting are greatly affected by applied pressure as the results show that at high specific pressure, the eutectic reaction of squeeze cast ZA27 alloy was restrained and a finer microstructure was obtained with the increase of pressure. similarly Zhu et al [3] Conducted experiments and simulations on the effect of pressure on porosity in cast A356. The alloy was melted under vacuum and pressure was applied in the ceramic mould and found that an increase in pressure reduces the amount of porosity and that the pore size distribution was shifted to smaller pores as pressure increased. Chiang et al [4] proposed mathematical models for the modeling and analysis of the effects of machining parameters on the performance characteristics in the high pressure die casting (HPDC) process of Al-Si alloys which were developed using the response surface methodology (RSM) to explain the influences of three processing parameters (die temperature, injection pressure and cooling time) on the performance characteristics of the mean particle size (MPS) of primary silicon and material hardness (HBN) value and found that two main factors involved in the mean particle size of primary silicon were the die temperature and the cooling time and that the injection pressure and die temperature also have statistically significant effect on microstructure and hardness, Dahle et al [5] conducted experiments on the effects of pressure on density and porosity in an aluminum cast by applying pressure to the riser in a permanent mold (die) and found a flat distribution. Dargusch et al [6] determined the effects of process variables on the quality of high pressure die cast components with the aid of in-cavity pressure sensors. In particular, the effects of set intensification pressure, delay time, and casting velocity were investigated and in turn the effect of variations in these parameters on the integrity of the final part, Porosity was found to decrease with increasing intensification pressure and increase with increasing casting velocity and then Sabau et al [7] developed a comprehensive methodology that takes into account solidification, shrinkage-driven inter-dendritic fluid flow, hydrogen precipitation, and porosity evolution for the prediction of the micro porosity fraction and distribution in aluminum alloy castings and found out that the effect of micro porosity on the inter-dendritic fluid flow cannot be neglected. This study is set out to look at the influence of pressure on the mechanical properties and grain refinement of die cast aluminium A1350 alloy.

## MATERIALS AND METHODS

The material that was used in this work is Aluminum A1350 (used mostly in electricity distribution lines) was procured, cut and melted in an electric furnace. The use of this alloy was because it was one of the most widely applied in the automotive and electrical industries.

The chemical composition of A1350 alloy as revealed by the x-ray fluorescence test is summarized in the table 1 below:

Table 1: Chemical composition of Aluminum A1350 alloy

|       | percentage composition |      |      |      |      |      |      |      |
|-------|------------------------|------|------|------|------|------|------|------|
|       | Al                     | Si   | Fe   | Cu   | Mn   | Cr   | Ni   | Zn   |
| A1350 | Bal                    | 0.01 | 0.40 | 0.05 | 0.01 | 1.80 | 0.01 | 0.05 |

## POURING AND MELTING

Aluminum A1350 was procured and melted in the electric furnace of capacity 500kg available at the scientific and equipment development institute, (SEDI), Enugu, Nigeria at a temperature of 720°C.

## PRESSURE APPLICATION

500 ton Cold chamber die casting machine available at the scientific and equipment development institute, (SEDI), Enugu, Nigeria was used to cast the samples. The injection pressure was regulated to permit a variety of pressure levels by a pressure regulating valve on the die cast machine and each phase of the experiment was described separately. Five specimen of the alloy were cast separately, The machine was operated at standard operating

conditions except the injection pressure which was varied at 0, 350, 700, 1050, and 1400kg/cm<sup>2</sup> for the experiment to allow for comparison of samples.

### DIES FOR EXPERIMENT

Since dies are very expensive to construct and build, dies used for the casting of top cylinders of vulcanizing machine available at the Scientific and Equipment Development Institute (SEDI), Enugu were used to cast the sample and specimen were cut from them for mechanical tests and microstructure analysis.



Figure 1: Samples of A1350 after casting

Table 2: Input parameters and their respective levels of the cast samples shown above

| Sample No (A1350) | Pouring temp °C | Injection pressure (Kg/cm <sup>2</sup> ) | Coating type | Cooling medium |
|-------------------|-----------------|--|--------------|----------------|
| 1                 | 720             | 1400                                     | graphite oil | Water + oil    |
| 2                 | 720             | 1050                                     | graphite oil | Water + oil    |
| 3                 | 720             | 700                                      | graphite oil | Water + oil    |
| 4                 | 720             | 350                                      | graphite oil | Water + oil    |
| 5                 | 720             | 0  | graphite oil | Water + oil    |

### RESULTS AND DISCUSSION

The results after casting 5 samples for the above factors are analyzed below:

#### HARDNESS test

The results obtained show variations in hardness values from 77 to 86 HRN with applied pressure and hardness is seen to increase as pressure increases from 350 to 1400kg/cm<sup>2</sup>. The experimental results show that pressure affects the hardness although not too significantly in the casting process. This result agrees with earlier work carried out by Ming et al [2] and Chiang et al [4]. The standard deviation was found to be  $S = 3.12409$ . The hardness follows this regression equation:

$$\text{Hardness}_{(A1350)} = 76.8 + 0.06287143 P, \quad \text{Where } P \text{ is Pressure}$$

Fig 2 below shows the graphical representations of hardness against casting pressure of A1350 alloy

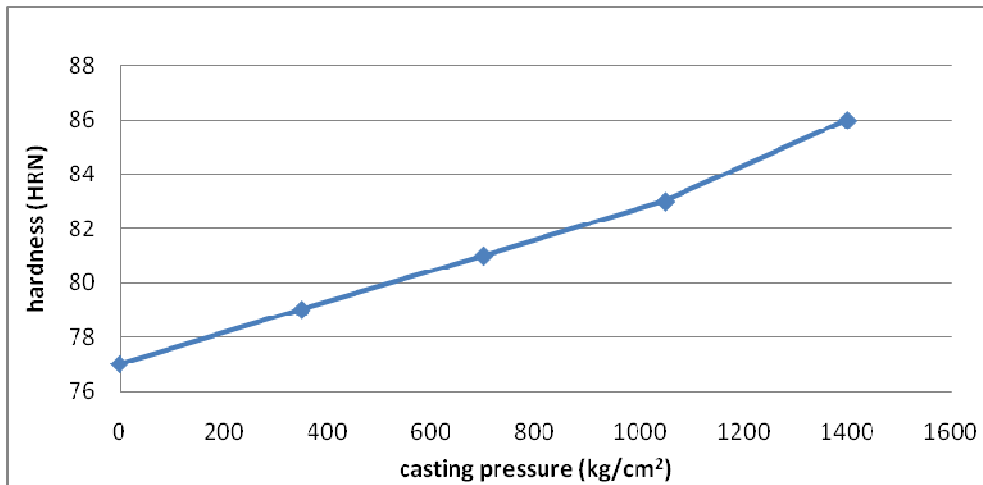


Figure 2: A plot of Hardness number against pressure of A1350

#### Tensile test

Fig 3 below shows the graphical representations of tensile strength against casting pressure of A1350 alloy.

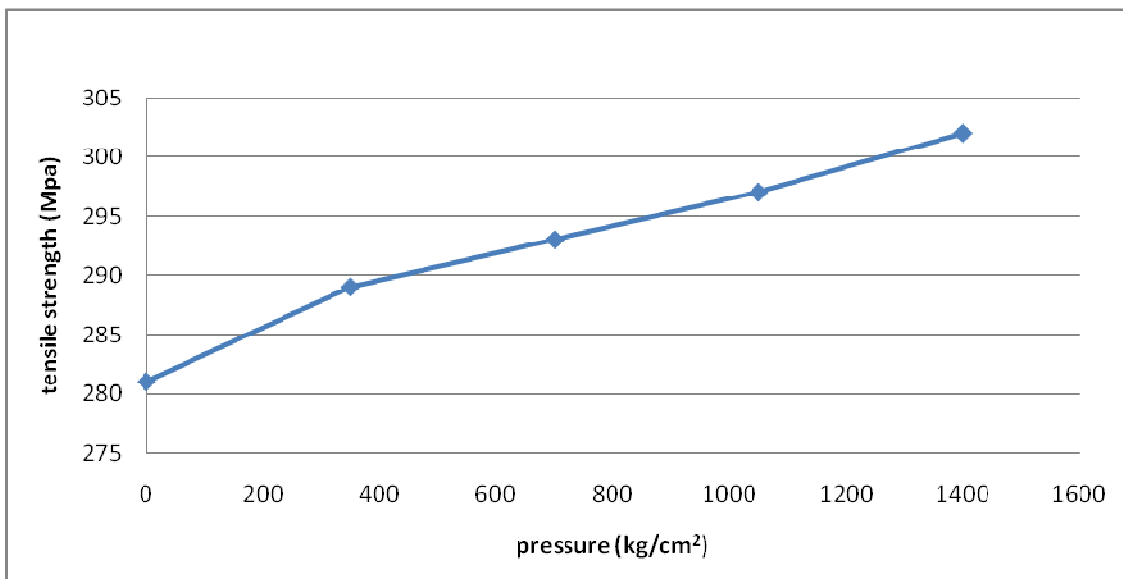


Figure 3: Tensile strength - pressure graph of A1350 alloy

The result shows variations also in the tensile strength of the samples with applied pressure as tensile strength increases from 280 to 302 MPa as casting pressure increased from 350 to 1400kg/cm<sup>2</sup>. with applied pressures indicating that pressure has effect on the tensile strengths in the casting process. These results also agree with those obtained by Ming et al [2]. The standard deviation was found to be  $S = 7.14423$ . The tensile strength follows this regression equation:

$$\text{Tensile strength}_{(A1350)} = 282.4 + 0.0142857143 P, \quad \text{Where } P \text{ is Pressure}$$

#### Yield test

Fig 4 below shows the graphical representations of yield strength against casting pressure of A1350 alloy.

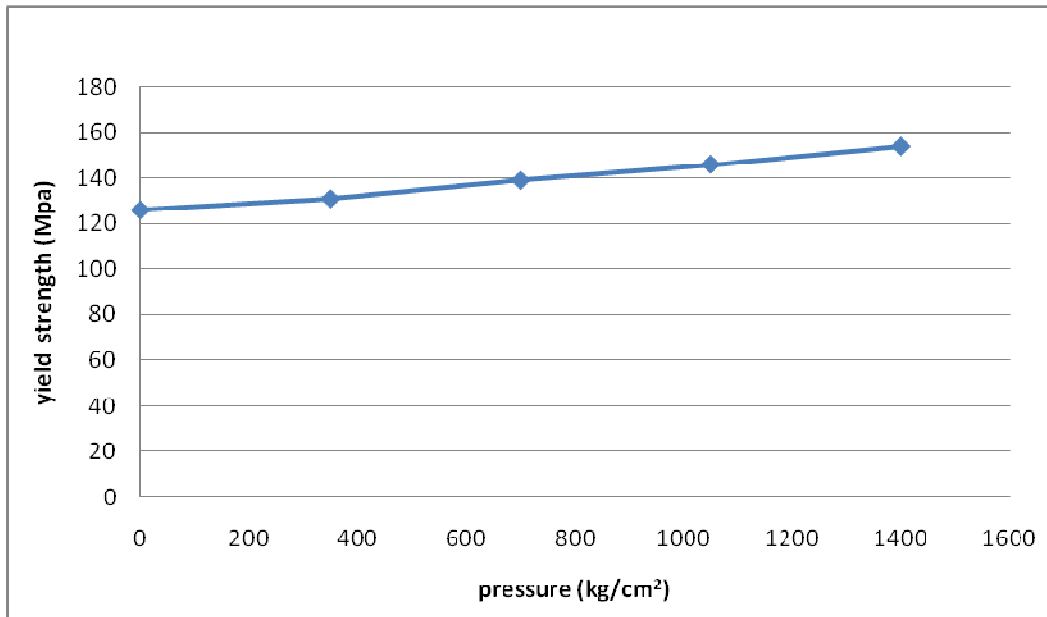


Figure 4: Yield strength - pressure graph of A1350 alloy

The results also shows variations in the yield strengths with applied pressure as graph shows that at pressures of 0kg/cm<sup>2</sup> to 1400kg/cm<sup>2</sup>, yield strength increases from 126 to 154 MPa. These results also agree with those obtained by Ming et al [2]. The standard deviation was found to be  $S = 10.06777$ . The yield strength follows this regression equation :

$$\text{Yield strength}_{(A1350)} = 125 + 0.0202857143 P, \quad \text{Where } P \text{ is Pressure}$$

**Impact test results**

Fig 5 below shows the graphical representations of impact energies against casting pressure of A1350 alloy.

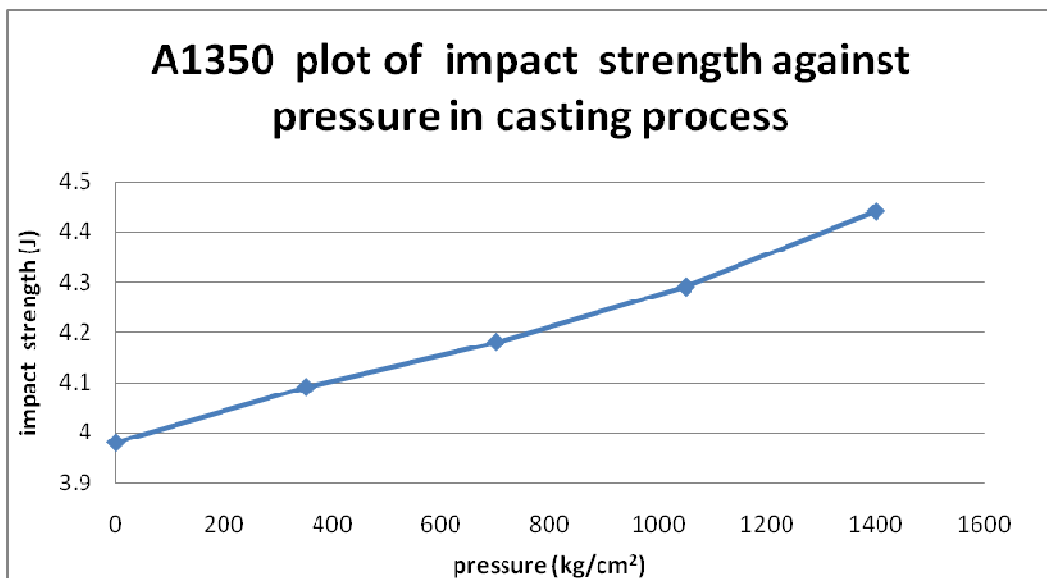


Figure 5: Impact strength - pressure graph of A1350 alloy

The results show similar variations in the impact strengths of the samples with impact strength increasing with increase in applied pressure. The experimental results show that pressure affects the impact strength of A1350 alloy. The standard deviation was found to be  $S = 0.15907$

The impact strength follows this regression equation :

$$\text{Impact strength}_{(A1350)} = 3.972 + 0.00032 P, \quad \text{Where } P \text{ is Pressure}$$

### NUMBER OF GRAINS

Fig 6 below shows the graphical representations of the number of grains against casting pressure of A1350 alloy.

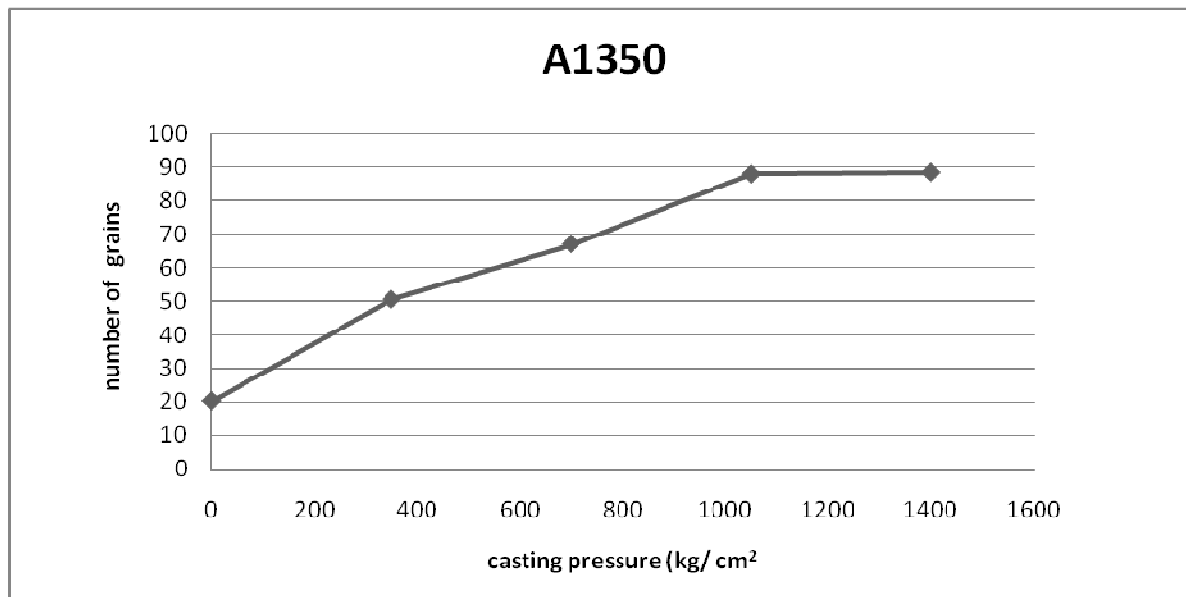


Figure 6: No of grains - pressure graphs of A1350 alloy

The number of grains were determined using the fully automated metallurgical microscope available at the metallurgy laboratory of the Federal University of Technology (FUTH) Minna, Nigeria which does digital image analysis and measures number of grains of the specimen per square inch and the result were recorded for each sample.

The number of grains were determined and presented as seen above in fig 6. The results show an increase in the number of grains with pressure. This result agrees with that obtained by ying-hui et al [8]. The standard deviation was found to be  $S = 25.62523$ . The number of grains follows this regression equation :

$$\text{Number of grains}_{(A1350)} = 28.078 + 0.04977 P, \quad \text{Where } P \text{ is Pressure}$$

### GRAIN SIZE

Fig 7 below shows the graphical representations of grain size against casting pressure of A1350 alloy.

The grain size of the samples are presented in fig 7 and shows a decrease in grain size with increase in casting pressure in the casting process. This result agrees with that obtained by ying-hui et al [7]. The standard deviation was found to be  $S = 1.72047$ . The grain size follows this regression equation:

$$\text{Grain Size} = 11.4 - 0.0045714P, \quad \text{where } P \text{ is Pressure}$$

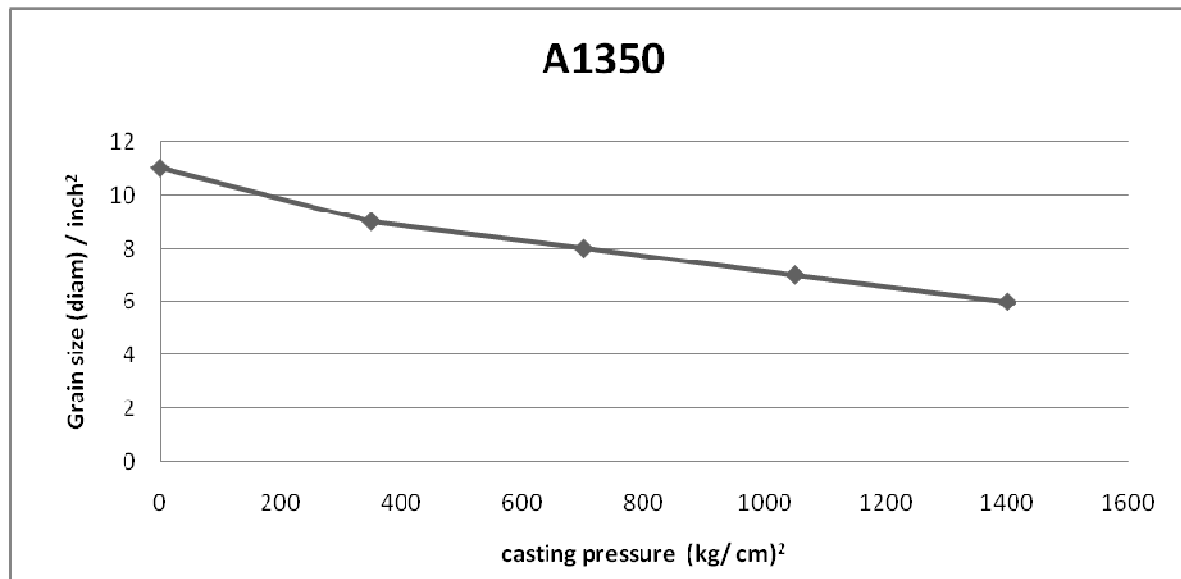


Figure 7: Grain size - pressure graphs of A1350 alloy

#### POROSITY MEASUREMENT

From the results obtained for the number of grains and grain size from the samples of A1350 alloy, simple analogy was deduced and porosity levels predicted in relation to the number of grains and grain size of the samples at the various injection pressures of the cast samples. The relation shows lower porosity at higher number of grains and finer grain sizes. This result agrees with work carried out by Dargusch et al, [6]. The regression was carried out using the multiple regression equation  $y = a + bx_1 + cx_2$

Where Y = porosity,  $X_1$  = grain size and  $X_2$  = number of grains. The porosity follows this regression equation:

$$Y_{(A1350)} = -0.69451 + 0.55546 X_1 - 0.011919 X_2$$

#### Metallographic Examination

Microstructures of the alloy samples were investigated by means of a scanning electron microscope available at the physics laboratory at Science and Technology Complex (SHEDA) Abuja, Nigeria and the metallurgical microscope available at metallurgy laboratory available at the Federal University of Technology (FUTH) Minna, Nigeria. Preparation of the samples for micro examination involved mainly sampling, polishing and etching. Samples measuring 26mm x15mm x 5mm were cut from the castings with the help of a hacksaw. The samples were filed and ground. Grinding was done in succession on a bench grinder using silicon carbide abrasive papers of 220-, 320-, 400-, and 600- grits, the specimen were polished in the usual manner with final polishing being carried out by hand, and they were etched in aqueous solution containing 2.5% HNO<sub>3</sub>, 1.5 % HCL and 1% HF acid (etched with Keller's reagent) for 20 to 60 seconds. Etching was done to make visible the grains of the samples under different pressures conditions.

#### Scanning Electron Microscope Analysis (SEM)

Microstructures of the samples were investigated by means of a scanning electron microscope (SEM) available at the physics laboratory at Science and Technology Complex (SHEDA) Abuja. Samples after preparation were placed to the multi-stub sample holder by the help of double sided conductive aluminum tape and mounted unto the sample chamber and an electron gun switched on which passed an accelerating voltage of 20kv and probe current of 227pA through the samples at a working distance of 6.0mm. SEM was done to make visible porosity pores across the microstructures of the samples under the different pressure conditions.

#### MICROSTRUCTURE ANALYSIS

The microstructures of the samples of A1350 alloy at the different applied pressures consisted of a primary  $\alpha$  phase, peritectic  $\beta$  phase and ternary eutectic ( $\beta+\eta+\epsilon$ ), where  $\alpha$  phases solidified as coarse grains (Fig.10). The primary  $\alpha$

phases became finer in higher pressure (seen in Figs 8 and 9) and with further increase of pressure, the microstructure became finer when the pressure reached  $1400 \text{ kg/cm}^2$  (seen in Fig. 8), however in the lower pressure samples, scanty grains were seen and were not homogeneously distributed across the micrograph (Fig. 10), also the eutectic structure ( $\beta+\eta+\epsilon$ ) was not found in the samples at  $1400 \text{ kg/cm}^2$ , while the hypo-eutectic ( $\eta+\epsilon$ ) phase appeared between grains (Fig. 8). in the solidification process, the primary phase  $\alpha$  precipitates first from liquid phase and then the peritectic reaction follows. However, at high pressure, the degree of these two reactions becomes greater due to the fact that the eutectic point moves to the direction of rich Al, thus the quantity of remaining liquid phase is reduced greatly. On the other hand, because the melting points are elevated at high pressure, the degree of super-cooling increases, thus the nucleate rate of primary reaction increases largely during solidifying and this is the reason of microstructure refining. In addition, the remaining phase is in deep super-cooling state when temperature is dropped to the eutectic point.

Therefore, the improvement of the mechanical properties was attributed to eliminating of micro-pores in the alloy caused by higher pressure. On the other hand, it is because of the microstructure refining as the applied pressure is increased as seen below that increased tensile strength and hardness are attributed. From the above results, it can be deduced that the eutectic reaction was restrained while the primary reaction was promoted at higher pressure. This viewpoint agrees with the results obtained by Ming et al [2], Ying- hui et al [8], and Zhu et al [3]

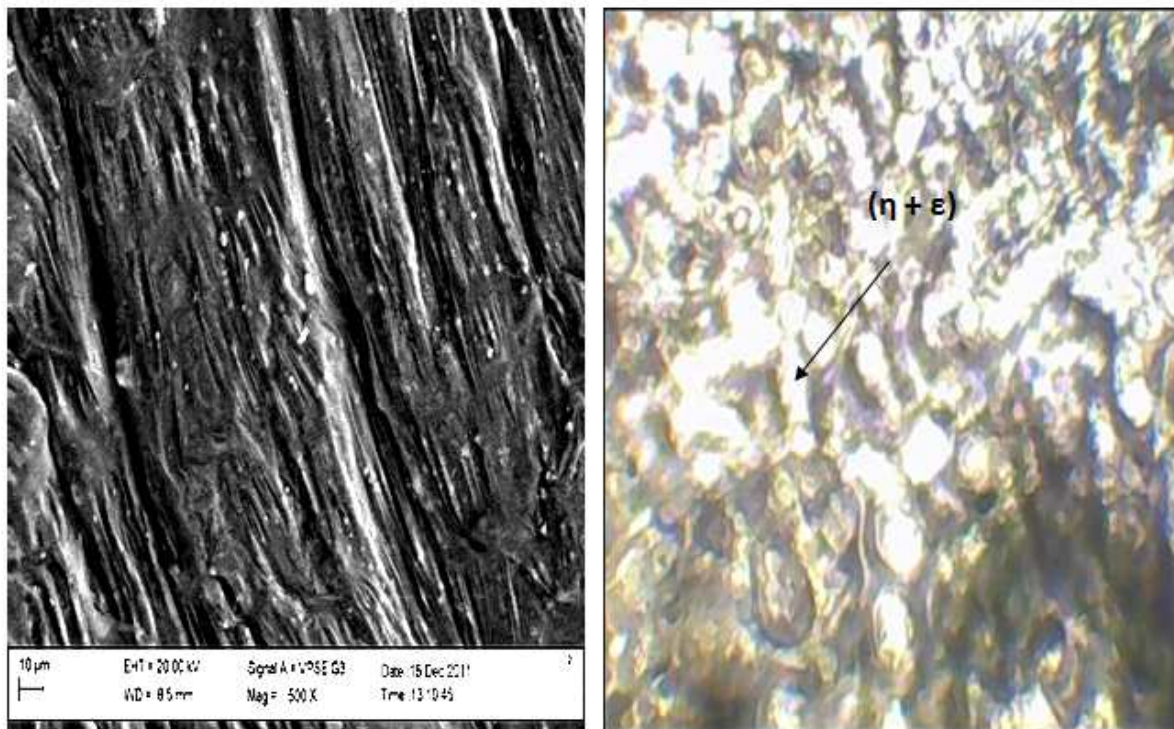


**Figure 8: Microstructure and Micrograph of sample 1 of Al350 with Injection pressure of  $1400 \text{ Kg/cm}^2$**

The microstructure of fig 8 shows fine grain structures that produced elongated pattern and the grains were finely and cohesively arranged and 95 percent or more of grains occupy the micrograph, also the micrograph shows ductile aluminum of transgranular surface due to good compatibility of the grain structures which is absolutely, evenly distributed in an attractive manner and perfectly embedded with one another. Also no pore was seen in the microstructure which would have indicated porosity.

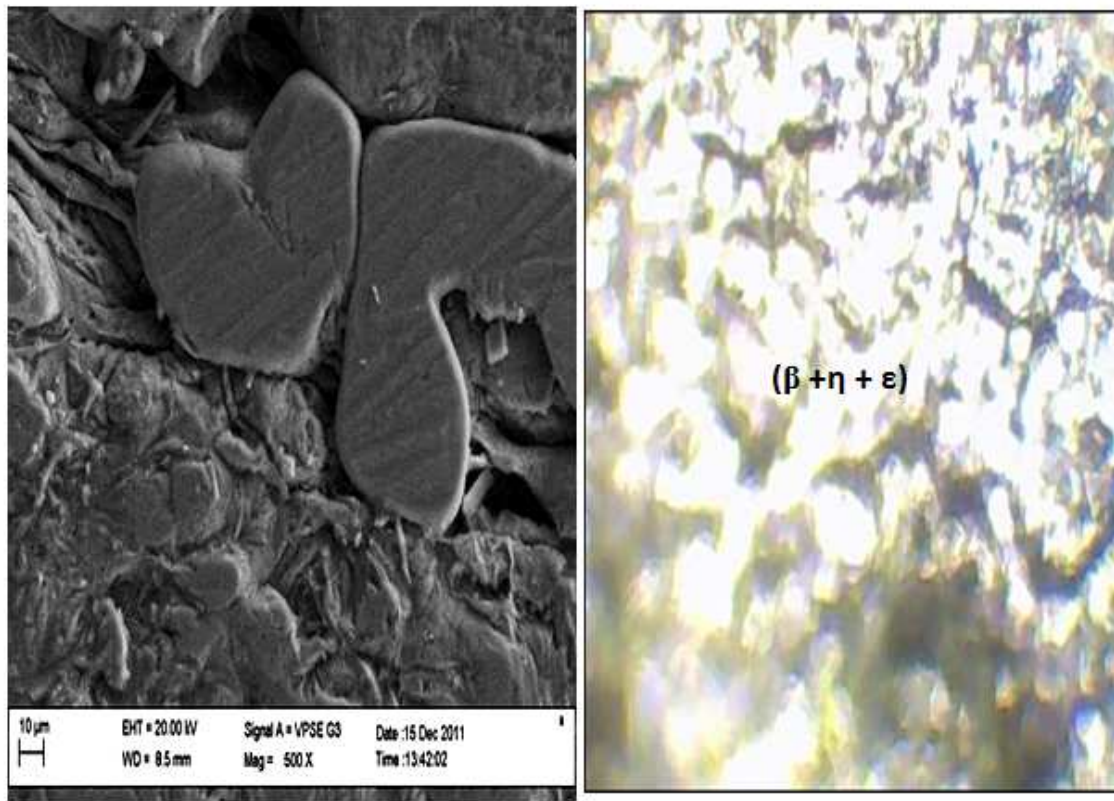


**Figure 9: Microstructure and Micrograph of sample 3 of Al350 with Injection**

**pressure of 700 Kg/cm<sup>2</sup>**

In fig 9, the microstructure shows that the grains are cohesively arranged and appear in a parabolic-shaped dimple characteristic appearance of the grains. The micrograph shows a ductile aluminum of a transgranular fracture surface. It also shows that almost 70 percent of grains occupy the micrograph, but leaving spaces which obviously shows not very fine grain sizes. Also no visible pore was seen in the microstructure which would have indicated porosity.

From the microstructure and micrograph of fig 10, it is seen that the grains are very scanty, also the regions at which grains occupies is about 30 percent of the micrograph. The microstructure and micrograph also shows deformation that is worsened and the degree of deformation so great. The grains clearly show no morphology that is obvious, probably due to low pressure. Also porosity will set in eventually due to poor quality of grains.

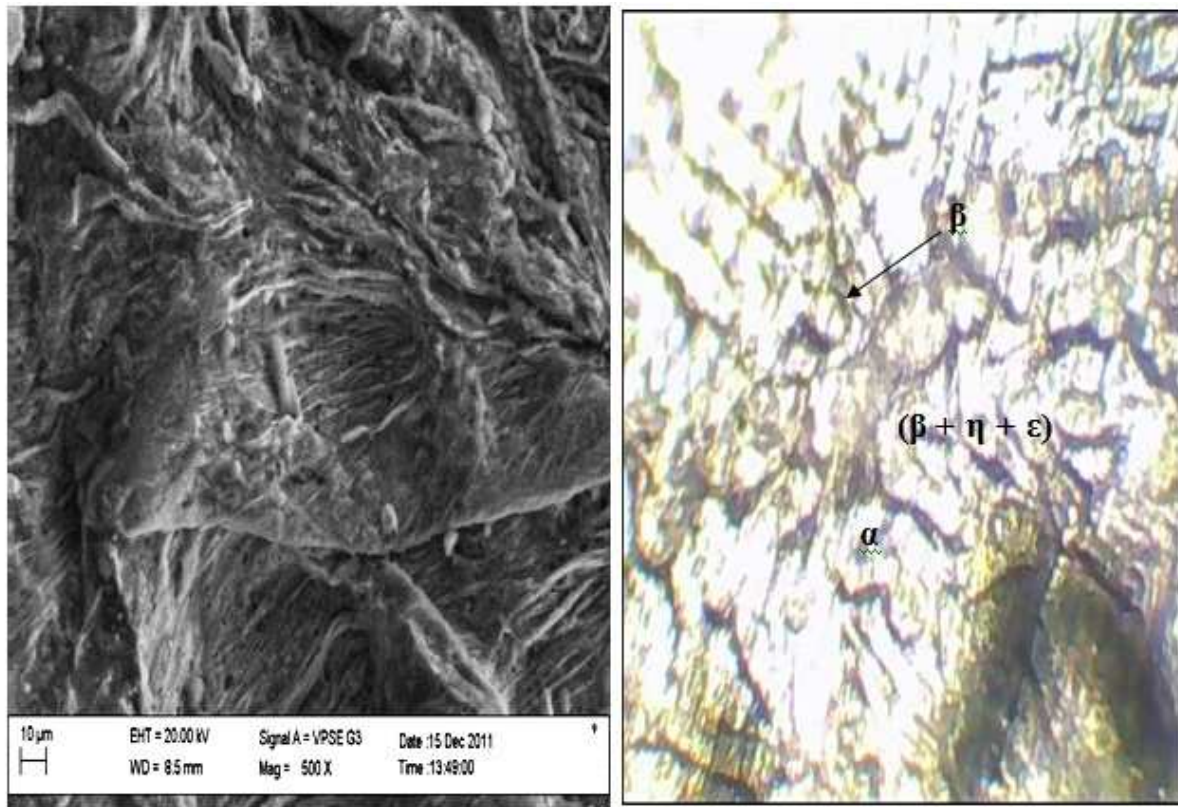


**Figure 10: Microstructure and Micrograph of sample5 of Al350 with Injection pressure of 0 Kg/cm<sup>2</sup>**

### CONCLUSION

From the results of this research, the following conclusions can be drawn:

- Number of grains of the samples showed variations with increasing applied pressure as more number of grains was seen in the microstructures at 1400kg/cm<sup>2</sup> pressure and few number of grains at zero pressure.
- Tensile, yield strength and elongation also varied across the different applied pressures in the samples as values were observed to increase with pressure.
- Microstructures of the samples show structural changes under the different applied pressures as some appear granular, lamellar, coarse e.t.c. It was seen that porosity susceptibility was obvious with decrease in pressure due to poor grains sizes and few number of grains and as no pore was seen on the micrographs and microstructure at 1400kg/cm<sup>2</sup> pressure. These trends confirm to the expected outcome.
- The impact strengths of the samples were also observed to vary with pressure in the casting process as they increased also with increase in applied pressure.
- The microstructures obtained from the samples at different pressures also shows that at 1400kg/cm<sup>2</sup> pressure, the eutectic reaction was restrained, and the final solidified structure was better signifying the influence of casting pressure, also the primary solid reaction ( $\alpha$ ) was promoted in the sample that solidified at 1400kg/cm<sup>2</sup> pressure and a finer microstructure was obtained .
- Hardness of the samples was observed to vary across the different applied pressures in the casting process as hardness values increased with applied pressure.
- The micrographs showed that different morphologies were distributed across the samples under the different applied pressures as finer grains which was homogenously distributed at 1400 kg/cm<sup>2</sup> pressure can effectively block the movement of dislocation, and the strength and plasticity increased.

## REFERENCES

- [1]NADCA, *About die casting* , the North American die casting association, archived from the original on <http://www.webcitation.org/5tVCFPCyL>, retrieved 2010-10-15 .
- [2] Ming, Z., Wei-wen, Z. , Hai-dong, Z. , Da-tong, Z. , Yuan-yuan, L. : *Transactions of Nonferrous Metals Society of China*, 2007 , 17, 3, 496–501.
- [3] Zhu J.D., Cockcroft S.L., and Maijer D.M., *Metallurgical and Materials Transactions A. Vol. 37A*. 2006 , pp.1075.
- [4]Chiang, Ko-Ta, Liu, Nun-Ming and Tsai Te-Chang. *Int J adv manuf technol* 2008 , 41, 1076-1084, springer-verlag london.
- [5]Dahle, A.K., Arnberg, L. and Apelian, D. : Burst Feeding and its Role in Porosity Formation During solidification of aluminum foundry alloys , 101st Casting Congress, American Foundry men’s Society, 1997 Seattle WA.
- [6]Matthew S, Dargusch, A., Dourb, G., Schauer, C., Dinnis, C.M. and Savaged, G. *Journal of Materials Processing Technology* 2006 , 180, 37-43.
- [7]Sabau A.S. and Vishvanathan S., *Metallurgical and Materials Transactions b Vol.33B*. 2002 , pp.243.
- [8]Ying-hui, W., Li Feng, H., Li-jing, Y., Bing-she, X., Munehiro, K., and Hideki, I. : *Journal of materials processing technology* 2009 , 209, 3278-3284.
- [9] Li, Rong-de, L., Zhong-ping, H., Yan-hua, B., Qing-sheng, Z., Hai-feng, Z. : *Foundry*, 2003 , 52, 3, 92–94.
- [10] Adler, L., Nagy, P. B., Rypien, D. V., and Rose, J. H. : Ultrasonic Evaluation of Porosity in Aluminium Cast Materials , Ohio State University, Columbus, OHIO, USA, 1989 .
- [11]Doehler, H., Art of and Apparatus for Casting Fluid Metal , United States Patent 973,483, United States Patent and Trademark Office, Washington D.C., 25, October 1910 .
- [12]Doehler, H., Die casting , McGraw hill book company, new York, 1951 .
- [13] Mikelonis, P. L., Walsh, L., Wurster, R., and Kimber, R. J. Marcel Dekker Foundry technology . In: *Quality Management Handbook*, eds.. new york, 1986 , pp. 753-790.
- [14] Shen-zhang, H., Zhen-peng, Z.: *special casting and nonferrous alloy*, 2002 , 22, 26–27. (in chinese).
- [15]Yoshihiko, H and Soichiro K. b., *Material and design* 30. 2009 , pp.1169-1173.
- [16]Yu, H. P, Zhang, F. Q, LI, R.D., *AFS transactions*, 1997 , 47, 689–692.